Published in final edited form as:
Biochemistry. 2011 February 15; 50(6): 1023–1028. doi:10.1021/bi1015315.

Nitric oxide dioxygenation reaction in DevS and the initial response to nitric oxide in *Mycobacterium tuberculosis*†

Erik T. Yukl[1,§], **Alexandra Ioanoviciu**[2], **Santhosh Sivaramakrishnan**[2], **Michiko M. Nakano**[1], **Paul R. Ortiz de Montellano**[2], and **Pierre Moënne-Loccoz**[1,*]

[1]Divison of Environmental & Biomolecular Systems, Oregon Health & Science University, 20,000 NW Walker Road, Beaverton, Oregon 97006-8921

[2]Department of Pharmaceutical Chemistry, University of California, 600 16th Street, San Francisco, California 94158-2517

Abstract

DevS and DosT from *Mycobacterium tuberculosis* (MTB) are paralogous heme-based sensor kinases that respond to hypoxia and to low concentrations of nitric oxide (NO). Both proteins work with the response regulator DevR as a two-component regulatory system to induce the dormancy regulon in MTB. While DevS and DosT are inactive when dioxygen is bound to the heme Fe(II) at their sensor domain, autokinase activity is observed in their heme Fe(II)-NO counterparts. To date, the conversion between active and inactive states and the reactivity of the heme-oxy complex toward NO have not been investigated. Here, we use stopped-flow UV-vis spectroscopy and rapid freeze quench resonance Raman to probe these reactions in DevS. Our data reveal that the heme-O_2 complex of DevS reacts efficiently with NO to produce nitrate and the oxidized Fe(III) heme through an NO dioxygenation reaction that parallels the catalytic reactions of bacterial flavohemoglobin and truncated hemoglobins. Autophosphorylation activity assays show that the Fe(III) heme state of DevS remains inactive, but exhibits high affinity for NO and forms an Fe(III)-NO complex that is readily reduced by ascorbate, a mild reducing agent. On the basis of these results, we conclude that upon exposure to low NO concentrations, the inactive oxy-heme complex of DevS is rapidly converted to the Fe(II)-NO complex in the reducing environment of living cells and triggers the initiation of dormancy.

Mycobacterium tuberculosis (MTB) is able to survive hypoxia and exposure to NO, conditions thought to be prevalent within the host (1,2), by undergoing a metabolic transformation to a state known as non-replicating persistence. Entrance into this state is characterized by the induction of a regulon of around 50 genes, the so-called “dormancy regulon” (3-5), and is regulated by the response regulator DevR of the two-component regulatory system known as DevSRT (alternatively DosSRT) (6). DevR is activated when the paralogous sensor kinases DevS and DosT autophosphorylate and subsequently transfer the phosphate group to DevR (7). DevS and DosT use a bound heme cofactor to sense environmental conditions and are inactive when the heme Fe(II) binds O_2. They become active when the heme is in the Fe(II) deoxy state, signaling hypoxia, or when it binds CO or NO (8-10). The Fe(III) state of DevS is also inactive (8,10), while the activity of this state in DosT has not been reported.

†This work was supported by Grants GM74785 (P.M.-L.) and AI074824 (P.R.O.M.) from the National Institutes of Health.

*Corresponding authors: Pierre Moënne-Loccoz, Oregon Health & Science University, 20,000 NW Walker Road, Beaverton, Oregon 97006. Tel: 503-748-1673; Fax: 503-748-1464. ploccoz@ebs.ogi.edu.
§Current address: Department of Biochemistry, Molecular Biology and Biophysics, University of Minnesota, Minneapolis, Minnesota 55455

Both sensors are required for wild-type levels of induction of the DevR regulon in response to both hypoxia (7) and NO exposure, as well as for survival (11) within the Wayne hypoxic model (2). Whether the effects of DevS and DosT are additive or whether they have specific roles in DevR activation is a question that has received significant attention. Two reports suggest that DevS acts as a redox sensor, whereas DosT is predominantly a sensor of hypoxia (8,12). These conclusions, which are based on high rates of autooxidation of the DevS oxy complex relative to that of DosT, suggest that DevS is present in the Fe(III) form under aerobic conditions and requires the action of a reducing agent upon transition into hypoxia. However, the reported rates of oxy-DevS autooxidation vary drastically. For example, one study reported that Fe(II) DevS converted directly to the Fe(III) form upon exposure to oxygen (8), whereas another determined a half life of 4.1 h at 37 °C for oxy-DevS (9), or even as high as 210 h at 25 °C when transition metal ions were removed from the medium (13). The latter study also identified an endogenous electron donor protein that could efficiently reduce ferric DevS. In view of the large differences in measured autooxidation rates, and the demonstration that DevS and DosT are intrinsically stable to autooxidation, it is highly speculative to differentiate the in vivo functions of DevS and DosT by their relative susceptibility to autooxidation.

An attractive hypothesis for the respective roles of DevS and DosT is that these two sensor kinases provide separate temporal activation of DevR, since DevS is expressed from the dormancy regulon controlled by DevR (5) while the expression level of DosT is unaffected by DevR or changes in O_2 concentrations (4,11,14). The inference is that DosT acts in the early response of MTB to NO exposure or hypoxia, thus upregulating expression of DevS for further response amplification. Indeed, analysis of dormancy regulon expression in DevS- and DosT-deletion strains, in response to anaerobic conditions, shows DosT to be responsible for ~60% of induction relative to wt after 4 h but only 7% after 6 days (11). In contrast, the response of each deletion mutant to NO was equivalent, with ~20% of induction relative to wt after 1 h aerobic incubation with NO donor. These data imply equivalent roles for DevS and DosT in NO signaling, with positive regulation of the dormancy regulon by PhoP leading to a basal level of DevS expression under aerobic conditions (11,15).

The ability of DevS and DosT to respond to NO under aerobic conditions is particularly interesting. The NO dioxygenation (NOD) reaction which converts NO to relatively harmless nitrate has been implicated as a major mechanism for relieving nitrosative stress in bacteria (16,17). This reaction is catalyzed by the oxy-heme groups of flavohemoglobins and truncated hemoglobins in bacteria as well as myoglobin and hemoglobin in mammals (18). In *Mycobacterium bovis*, a truncated hemoglobin HbN possesses NOD activity and confers NO resistance (19). The HbN homologue of MTB performs the same function when expressed in heterologous hosts (20). Although DevS and DosT are unlikely to function catalytically as detoxification enzymes, the NOD reaction could provide a mechanism for termination of the kinase inhibition imposed by the ferrous dioxy complex.

Materials and Methods

Protein Expression and Purification

Full-length DevS and DosT were obtained as a His-tagged construct as described in (21). Activity and spectroscopy measurements on full-length DevS were unchanged by the presence of the His-tag, but removal by TEV protease was required with full-length DosT as the presence of this tag was previously observed to affect the ligation and spin states of the Fe(II) heme.[2]

Protein and NO Solutions

Protein solutions were prepared in 50 mM phosphate buffer pH 7.5 with 150 mM NaCl and purged with argon before being brought into a glovebox with a controlled atmosphere of less than 1 ppm O_2 (Omni-Lab System, Vacuum Atmospheres Co.). Reduction to the heme Fe(II) protein was achieved by addition of a 5-fold excess of sodium dithionite followed by passage through a Sephadex G-25 desalting column (GE Healthcare). Complete heme reduction and dithionite removal were confirmed by UV-vis spectroscopy with a Cary 50 spectrometer. Solutions were then transferred to sealed serum bottles and exposed to $^{16}O_2$ (Airgas). Formation of oxy complex was confirmed by UV-vis spectroscopy and the final protein concentration was determined. The serum bottles were then opened in the glovebox to release excess O_2 prior to loading the protein solution in rapid-freeze quench (RFQ) syringes or gas-tight Hamilton syringes for transfer to the stopped-flow apparatus. For RFQ experiments, $^{14}N^{16}O$ (Airgas) and $^{15}N^{16}O$ (98% ^{15}N, 95% ^{16}O, Aldrich) solutions were prepared by serial additions of NO gas into a sealed vial of anaerobic buffer. Concentrations of NO in stock solutions were determined by titration with deoxymyoglobin. Solutions in sealed serum bottles were drawn into RFQ syringes using a needle attachment within the glovebox. For stopped-flow experiments, a concentrated solution of diethylamine NONOate (Cayman Chemical) (8.7 mM) was diluted in anaerobic phosphate buffer and incubated for 1 h at room temperature within the Hamilton gas-tight syringe prior to loading into the stopped-flow apparatus.

Nitrate/nitrite concentrations measurements

Nitrate and nitrite productions from the reaction of oxy-DevS with NO were measured using the Griess reagent and nitrite reductase (nitrate/nitrite colorimetric kit by Cayman Chemical). Specifically, saturated NO solutions were used to reach a final NO concentration of 30 μM in solutions of oxy-DevS and oxy-myoglobin ranging between 6 and 9 μM and in buffer blanks. Complete conversion of oxy-DevS to oxidized Fe(III) DevS was confirmed by UV-vis spectroscopy and matched the nitrate concentration deduced from the colorimetric measurement.

Autophosphorylation Assays

DevS and DosT protein solutions in 50 mM potassium phosphate buffer at pH 7.5 with 100 mM NaCl were purged with Ar and reduced with sodium dithionite. Excess dithionite was removed using desalting columns and CO or O_2 gas was added to appropriate samples. Fully-oxidized Fe(III) protein solutions were obtained from incubation in 2 mM potassium ferricyanide followed by desalting using spin columns (Zebra, Pierce). NO gas was added to these samples directly prior to addition of ATP to generate the Fe(III)-NO complex. As an alternative route to the production of the Fe(III)-NO complex, NONOate was used to produce a 3-fold excess of NO. These operations were performed in the anaerobic glove box. All samples, except the oxy and Fe(III) proteins, were loaded into septum-sealed microcentrifuge tubes. All 50 μL assay samples contained final concentrations of 5.0 μM protein, 100 mM Tris-HCl pH 7.5, 50 mM KCl, and 5 mM $MgCl_2$, after ATP addition. The CO samples also included 500 μM sodium dithionite. Reactions were initiated by syringe addition of a few μL of a solution containing $\gamma^{32}P$ ATP (4500 Ci/mmol) (MP Biomedicals) and Ar-purged, unlabeled ATP (Sigma) to a final concentration of 500 μM and 5-10 μCi. Our earlier work used a final ATP concentration of 200 μM and 10 μCi (10), but the higher ATP concentrations used in this study result in a significant increase in final autophosphorylation levels. 10 μL aliquots were removed at various time points and combined with 3.0 μL stop buffer (208 mM Tris-HCl pH 6.8, 8.3% SDS, 42% glycerol, 167

[2]Yukl, E. T., Ioanoviciu, A., Sivaramakrishnan, S., Ortiz de Montellano, P. R. and Moënne-Loccoz, P. (2010). Unpublished results.

mM DTT, and 0.08% bromophenol blue). These samples were run through a 12% polyacrylamide gel, which was vacuum-dried at 80 °C for 1.5 h, and exposed in a PhosphorImager cassette (Molecular Dynamics) for approximately 24 to 48 h. Levels of phosphorylated protein were imaged on a Typhoon Trio+ PhosphorImager (Amersham Biosciences) and quantified according to Nakamura et al. (22) except that the 1.65 correction factor was eliminated since gels were completely dried. After exposure, dried gels were rehydrated in 20% methanol 5% acetic acid solution and Coomassie stained to confirm consistency in amount of protein loaded and integrity of full length proteins.

Stopped-Flow UV-vis Spectroscopy

Oxy-DevS, Oxy-DosT, and NO solutions were generated as described above and loaded into a SX20 stopped-flow UV-vis spectrometer (Applied Photophysics) equipped with a photodiode array detector and a water bath equilibrated to 4.2 °C to collect spectral data from 4 ms to 4 s. The purity of oxy-form of the enzymes was confirmed by UV-vis spectroscopy prior to loading into the stopped flow instrument; excess solutions in the loading syringes were recovered from the stopped-flow apparatus after the experiments to confirm the stability of the oxy complexes in the absence of NO.

Rapid Freeze Quench (RFQ)

Solutions were generated as described above and were loaded into the System 1000 Chemical / Freeze Quench Apparatus (Update Instruments, Inc.) equipped with a water bath maintained at 3-4 °C. Reaction times were controlled by varying the syringe displacement rate from 2-8 cm/s or by varying the volume of the reactor hose after the mixer. 5 ms were added to the calculated reaction times to account for time of flight and freezing in liquid ethane. Samples of 250 μL were ejected into a glass funnel attached to EPR tubes filled with liquid ethane at ≤ -120° C. The frozen sample was packed into the tube as the assembly sat within a Teflon block cooled with liquid nitrogen to ≤ -100° C. Liquid ethane was removed by immersing tubes in ethanol cooled to ~ -100° C and applying vacuum for 5 – 10 min. Resonance Raman (RR) analysis before and after cryosolvent removal showed no perturbation in spectra due to this treatment. Successful mixing and NO dioxygenation reaction was confirmed by UV-vis analysis of samples ejected into a microcentrifuge tube, and by RR analysis of samples shot into a room temperature NMR tube and frozen manually. These manually frozen samples and resting Fe(II)O_2, Fe(III), and Fe(III)NO were used to acquire low-temperature RR spectra of resting states for comparison with spectra of RFQ samples.

RR Spectroscopy

Low temperature RR spectra were obtained using a backscattering geometry on RFQ samples and control samples in EPR tubes maintained at ~ 105 K in a liquid nitrogen cold finger. All spectra were collected on a custom McPherson 2061/207 spectrograph (0.67 m with variable gratings) equipped with a Princeton Instruments liquid N2-cooled CCD detector (LN-1100PB) as described previously. Excitation at 413 nm was provided by a krypton laser (Innova 302, Coherent), and a Kaiser Optical supernotch filter was used to attenuate Rayleigh scattering. Frequencies were calibrated relative to indene and CCl_4 and are accurate to ±1 cm^{-1}.

Results and Discussion

Stopped-flow analyses of the reactions of oxy-DevS with substoichiometric NO show conversion of the oxy complexes to Fe(III) hemes (Figure 1). Specifically, while the initial oxy-DevS solution exhibits characteristic absorptions at 414, 541, and 577 nm (see Materials and Methods), the first stopped-flow trace obtained 4 ms after mixing of oxy-

DevS with NO, and subsequent traces, show a decrease of these absorbance features in favor of a Soret maximum at 407 nm and absorption at 498 and 632 nm that are consistent with formation of Fe(III)-DevS. Despite our efforts to maximize the anaerobicity of the stopped-flow instrument, reproducing precise NO concentrations in the low micromolar range was unworkable in the absence of an anaerobic chamber confining the apparatus. Consequently, NO concentrations were inferred from the amount of oxy-complex consumed after mixing. At 2 μM NO, the rate of the reaction with oxy-DevS at pH 7.5 was observed to be biphasic with k_{obs} = 36 s^{-1} and 1.2 s^{-1} (Figure 1). Analysis of total nitrate and nitrite concentrations confirm quantitative conversion of NO to NO_3^- by oxy-DevS (data not shown), as observed previously for oxymyoglobin and *M. bovis* HbN (19). Thus, in spite of technical limitations preventing adequate measurements to determine second order rate constants of this reaction, the existing results clearly demonstrate efficient NOD reactivity in the sensor kinase DevS.

The NOD reaction in DevS was also monitored by RFQ and RR spectroscopy, techniques that we have used together successfully to trap and characterize an Fe(III)-nitrato complex in the NOD reaction of myoglobin at pH 9.5 (23). The high-frequency RR spectra of 300 μM oxy-DevS mixed with excess NO and frozen at 7, 15, and 55 ms are nearly identical to that of the oxy-complex (Figure 2). Specifically, the porphyrin ν_4, ν_3, ν_2, and ν_{10} modes are observed at 1374, 1501, 1581 and 1640 cm^{-1}, respectively, and are characteristic of six-coordinate low-spin (6cLS) Fe(III) heme species (24). In contrast, the Fe(III) heme of DevS is predominantly 6cHS with ν_4, ν_3, and ν_{10} at 1370, 1478, and 1617 cm^{-1}, respectively.

The low-frequency RR spectra of the RFQ samples show a rapid consumption of the oxy complex, as determined by the loss of the ν(Fe-O_2) at 566 cm^{-1} in the 7-ms RFQ sample (Figure 3); This mode was previously observed at 563 cm^{-1} in wt DevS at room temperature (10,25). The loss of the ν(Fe-O_2) band is accompanied by the gradual appearance of a mode at 601 cm^{-1}, which downshifts by − 5 cm^{-1} when the NO solution is substituted with ^{15}NO (Figure 3). The observed frequency and ^{15}N-isotope shift are consistent with the assignment of this mode to a ν(Fe-NO) from an Fe(III)-NO complex (26-28). These assignments are consistent with the RR spectra of resting oxy-DevS, Fe(III)-DevS, and Fe(III)-NO DevS (Figure 3). Thus, the RR spectra of the RFQ samples provide evidence for the rapid decay of the oxy complex upon its reaction with excess NO to generate an Fe(III) state that can further react with excess NO to form a stable Fe(III)-NO complex.

The RFQ-RR data suggest that Fe(III) DevS has an unusually high affinity for NO, and indeed, titration of an anoxic solution of Fe(III) DevS with a solution of NO yields an apparent K_d of ~ 5 μM (Figure 4A). This unusually high NO affinity exhibited by an Fe(III) heme protein (28) suggests that the Fe(III)-NO state could be physiologically relevant in the infected macrophage. The Fe(III)-NO complex of DevS shows only marginal activity in autophosphorylation assays compared to oxy-DevS (Figure 5) (8), but we have found that the Fe(III)-NO complex is easily reduced with 10 mM ascorbate, i.e., about 20-fold faster than the Fe(III) DevS state (Figure 4B). Thus, reduction of the Fe(III)-NO complex to Fe(II)-NO can be expected to be a rapid process in the reducing cellular environment and would lead to the activation of the kinase domain. As such, the NOD reaction of oxy-DevS may represent a rapid switching mechanism to convert an inactive oxy state to an active Fe(II)-NO species via formation of the Fe(III) and Fe(III)-NO DevS states (Figure 6).

Given the possible early sensing role of DosT, the reactivity of its oxy form with NO and the NO affinity of its Fe(III) state are also of interest. Preliminary stopped-flow monitoring of the reaction of oxy-DosT with NO (at 0.57 μM) revealed a monophasic reaction with k_{obs} ~ 1 s^{-1} similar to the slower component of the biphasic rate observed in DevS (data not shown), but no further stopped-flow experiments were carried out with DosT because activity measurements revealed poor stability of the DosT protein. Instability of

ferricyanide-oxidized DosT and its tendency to precipitate also prevent an accurate assessment of its affinity for NO. Despite problems of stability with DosT, the efficiency of the reaction of oxy-DosT with NO in aerobic conditions could be documented using the slow NO donor DEA-NONOate (Figure 7). Specifically, as a first equiv of NO is produced, the conversion of oxy-DosT to the Fe(III) state is confirmed by the decrease in Soret absorption at 413 nm and the loss of well-resolved α/β bands a 578 and 543 nm in favor of the less distinctive absorption features of the oxidized protein (Figure 7A). Subsequent production of NO beyond 1 equiv results in an increased Soret absorption at 419 nm (Figure 7B), an observation consistent with partial conversion of the Fe(III) state to Fe(III)-NO despite the competing reaction of molecular oxygen with NO. The amount of Fe(III)-NO formed in these experiments suggest an upper limit of 1 μM for the K_d in Fe(III) DosT.

Conclusion

Previous studies have shown that the complexes of CO and NO with ferrous DevS and DosT activate the autophosphorylation that eventually leads to induction of the dormancy regulon. In contrast, the dioxygen complex has negligible autophosphorylation activity (8-10). Ferric DevS, like the dioxygen complex, does not significantly autophosphorylate, but the ligand-free ferrous form exhibits intermediate autophosphorylation activity. Thus, one mechanism for induction of the dormancy regulon includes a transition to a sufficiently low O_2 tension such that the ferrous protein is unliganded or competitively coordinated by CO. The situation with NO differs, since NO has potent anti-mycobacterial properties, and exposure to this gas can occur abruptly, requiring a rapid response. The present results suggest that NO initiates a dormancy response not by exchanging with oxygen as the ligand to the heme Fe(II), but rather by reacting with the Fe(II)-O_2 complex to produce a heme Fe(III) or heme Fe(III)-NO complex, if the concentration of NO is in the micromolar range. Both Fe(III) and Fe(III)-NO states can be subsequently reduced to the Fe(II) and Fe(II)-NO states. We have previously identified a redox partner in *M. tuberculosis* that can reduce ferric DevS to the ferrous state and can therefore presumably also reduce the ferric NO complex. In this regard, it is useful to note that the Fe(III)-NO form is much more easily reduced by ascorbate than the unliganded Fe(III) form. Since the Fe(II)-NO complex is highly activated for autophosphorylation (8-10), the net result of the exposure of DevS-O_2 to NO is a rapid initiation of the dormancy response.

References

1. Choi HS, Rai PR, Chu HW, Cool C, Chan ED. Analysis of nitric oxide synthase and nitrotyrosine expression in human pulmonary tuberculosis. Am J Respir Crit Care Med. 2002; 166:178–186. [PubMed: 12119230]
2. Wayne LG, Sohaskey CD. Nonreplicating persistence of *mycobacterium tuberculosis*. Annu Rev Microbiol. 2001; 55:139–163. [PubMed: 11544352]
3. Cunningham AF, Spreadbury CL. Mycobacterial stationary phase induced by low oxygen tension: cell wall thickening and localization of the 16-kilodalton -crystallin homolog. J Bacteriol. 1998; 180:801–808. [PubMed: 9473032]
4. Sherman DR, Voskuil M, Schnappinger D, Liao R, Harrell MI, Schoolnik GK. Regulation of the *Mycobacterium tuberculosis* hypoxic response gene encoding alpha -crystallin. Proc Natl Acad Sci U S A. 2001; 98:7534–7539. [PubMed: 11416222]
5. Voskuil MI, Schnappinger D, Visconti KC, Harrell MI, Dolganov GM, Sherman DR, Schoolnik GK. Inhibition of respiration by nitric oxide induces a *Mycobacterium tuberculosis* dormancy program. J Exp Med. 2003; 198:705–713. [PubMed: 12953092]
6. Dasgupta N, Kapur V, Singh KK, Das TK, Sachdeva S, Jyothisri K, Tyagi JS. Characterization of a two-component system, devR-devS, of *Mycobacterium tuberculosis*. Tuber Lung Dis. 2000; 80:141–159. [PubMed: 10970762]

7. Roberts DM, Liao RP, Wisedchaisri G, Hol WG, Sherman DR. Two sensor kinases contribute to the hypoxic response *of Mycobacterium tuberculosis*. J Biol Chem. 2004; 279:23082–23087. [PubMed: 15033981]
8. Kumar A, Toledo JC, Patel RP, Lancaster JR Jr, Steyn AJC. *Mycobacterium tuberculosis* DosS is a redox sensor and DosT is a hypoxia sensor. Proc Natl Acad Sci USA. 2007; 104:11568–11573. [PubMed: 17609369]
9. Sousa EH, Tuckerman JR, Gonzalez G, Gilles-Gonzalez MA. DosT and DevS are oxygen-switched kinases in *Mycobacterium tuberculosis*. Protein Sci. 2007; 16:1708–1719. [PubMed: 17600145]
10. Yukl ET, Ioanoviciu A, Nakano MM, de Montellano PR, Moënne-Loccoz P. A distal tyrosine residue is required for ligand discrimination in DevS from *Mycobacterium tuberculosis*. Biochemistry. 2008; 47:12532–12539. [PubMed: 18975917]
11. Honaker RW, Leistikow RL, Bartek IL, Voskuil MI. Unique roles of DosT and DosS in DosR regulon induction and *Mycobacterium tuberculosis* dormancy. Infect Immun. 2009; 77:3258–3263. [PubMed: 19487478]
12. Cho HY, Cho HJ, Kim YM, Oh JI, Kang BS. Structural insight into the heme-based redox sensing by DosS from *Mycobacterium tuberculosis*. J Biol Chem. 2009; 284:13057–13067. [PubMed: 19276084]
13. Ioanoviciu A, Meharenna YT, Poulos TL, Ortiz de Montellano PR. DevS oxy complex stability identifies this heme protein as a gas sensor in *Mycobacterium tuberculosis* dormancy. Biochemistry. 2009; 48:5839–5848. [PubMed: 19463006]
14. Saini DK, Malhotra V, Tyagi JS. Cross talk between DevS sensor kinase homologue, Rv2027c, and DevR response regulator of *Mycobacterium tuberculosis*. FEBS Lett. 2004; 565:75–80. [PubMed: 15135056]
15. Gonzalo-Asensio J, Mostowy S, Harders-Westerveen J, Huygen K, Hernandez-Pando R, Thole J, Behr M, Gicquel B, Martin C. PhoP: a missing piece in the intricate puzzle of *Mycobacterium tuberculosis virulence*. PLoS ONE. 2008; 3:e3496. [PubMed: 18946503]
16. Poole RK, Hughes MN. New functions for the ancient globin family: bacterial responses to nitric oxide and nitrosative stress. Mol Microbiol. 2000; 36:775–783. [PubMed: 10844666]
17. Brunori M. Nitric oxide moves myoglobin centre stage. Trends Biochem Sci. 2001; 26:209–210. [PubMed: 11295538]
18. Gardner PR. Nitric oxide dioxygenase function and mechanism of flavohemoglobin, hemoglobin, myoglobin and their associated reductases. J Inorg Biochem. 2005; 99:247–266. [PubMed: 15598505]
19. Ouellet H, Ouellet Y, Richard C, Labarre M, Wittenberg B, Wittenberg J, Guertin M. Truncated hemoglobin HbN protects *Mycobacterium bovis* from nitric oxide. Proc Natl Acad Sci U S A. 2002; 99:5902–5907. [PubMed: 11959913]
20. Pathania R, Navani NK, Gardner AM, Gardner PR, Dikshit KL. Nitric oxide scavenging and detoxification by the *Mycobacterium tuberculosis* haemoglobin, HbN in *Escherichia coli*. Mol Microbiol. 2002; 45:1303–1314. [PubMed: 12207698]
21. Ioanoviciu A, Yukl ET, Moënne-Loccoz P, Ortiz de Montellano PR. DevS, a heme-containing two-component oxygen sensor of *Mycobacterium tuberculosis*. Biochemistry. 2007; 46:4250–4260. [PubMed: 17371046]
22. Nakamura H, Saito K, Shiro Y. Quantitative measurement of radioactive phosphorylated proteins in wet polyacrylamide gels. Anal Biochem. 2001; 294:187–188. [PubMed: 11444816]
23. Yukl ET, de Vries S, Moënne-Loccoz P. The millisecond intermediate in the reaction of nitric oxide with oxymyoglobin is an iron(III)-nitrato complex, not a peroxynitrite. J Am Chem Soc. 2009; 131:7234–7235. [PubMed: 19469573]
24. Spiro, TG.; Li, XY. Resonance Raman spectroscopy of metalloporphyrins. In: Spiro, TG., editor. In Biological Applications of Raman Spectroscopy Vol 3 Resonance Raman spectra of hemes and metalloproteins. John Wiley & Sons; New York: 1988. p. 1-37.
25. Yukl ET, Ioanoviciu A, de Montellano PR, Moënne-Loccoz P. Interdomain interactions within the two-component heme-based sensor DevS from *Mycobacterium tuberculosis*. Biochemistry. 2007; 46:9728–9736. [PubMed: 17676768]

26. Benko B, Yu NT. Resonance Raman studies of nitric oxide binding to ferric and ferrous hemoproteins: detection of Fe(III)-NO stretching, Fe(III)-N-O bending, and Fe(II)-N-O bending vibrations. Proc Natl Acad Sci U S A. 1983; 80:7042–7046. [PubMed: 6580627]

27. Mukai M, Ouellet Y, Ouellet H, Guertin M, Yeh SR. NO binding induced conformational changes in a truncated hemoglobin from *Mycobacterium tuberculosis*. Biochemistry. 2004; 43:2764–2770. [PubMed: 15005611]

28. Wang J, Lu S, Moënne-Loccoz P, Ortiz de Montellano PR. Interaction of nitric oxide with human heme oxygenase-1. J Biol Chem. 2003; 278:2341–2347. [PubMed: 12433915]

Abbreviations

MTB	*Mycobacterium tuberculosis*
wt	wild-type
NOD	nitric oxide dioxygenation reaction
RR	resonance Raman
EPR	electron paramagnetic resonance
FTIR	Fourier transform infra-red
RFQ	rapid freeze quench
HS/LS	high-spin/low-spin

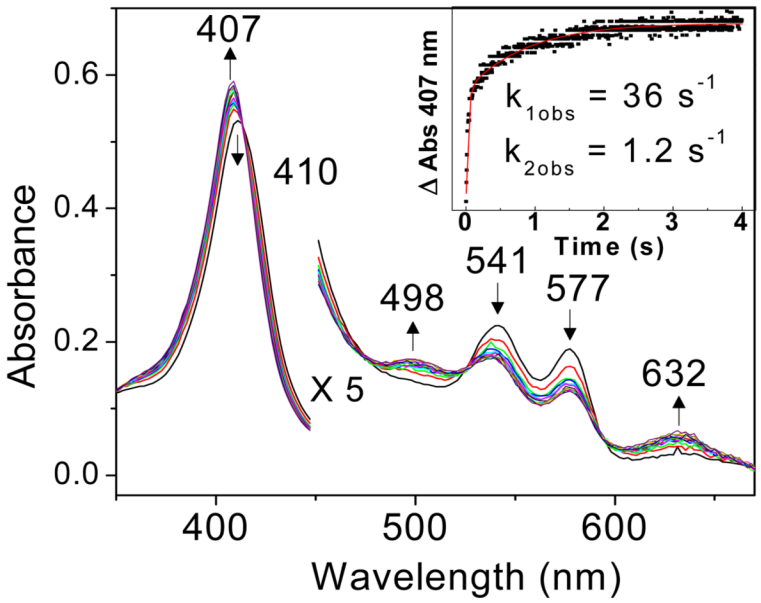

Figure 1.

Stopped-flow UV-vis absorption spectra of the reaction of 4 μM oxy-DevS with 2 μM NO at 4.2 °C and pH 7.5. Inset: kinetics of the reaction measured at 407 nm.

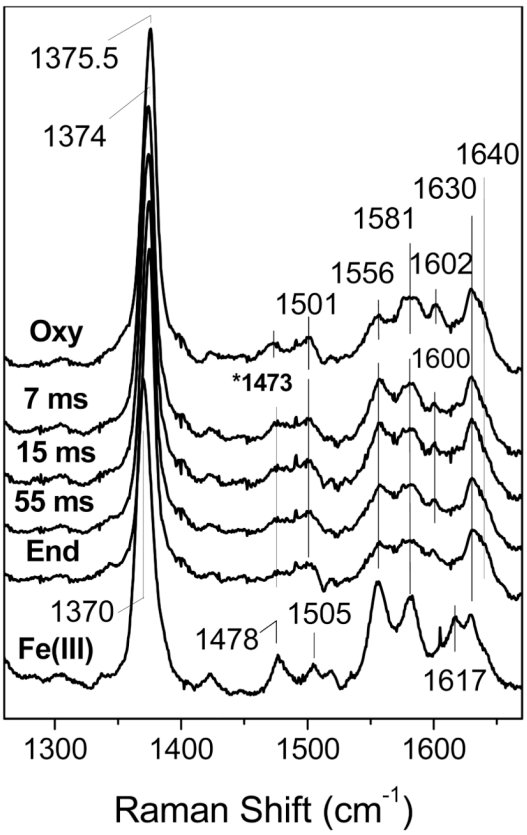

Figure 2.

High-frequency RR spectra of RFQ samples of the reaction of 300 μM oxy-DevS with excess NO compared to those of resting oxy- (top trace) and Fe(III)-DevS (bottom trace). (λ_{exc} = 413 nm, 20 mW; sample temperature ~ 105 K). The 1473 cm^{-1} Raman band in the spectra of RFQ samples is assigned to residual frozen ethane.

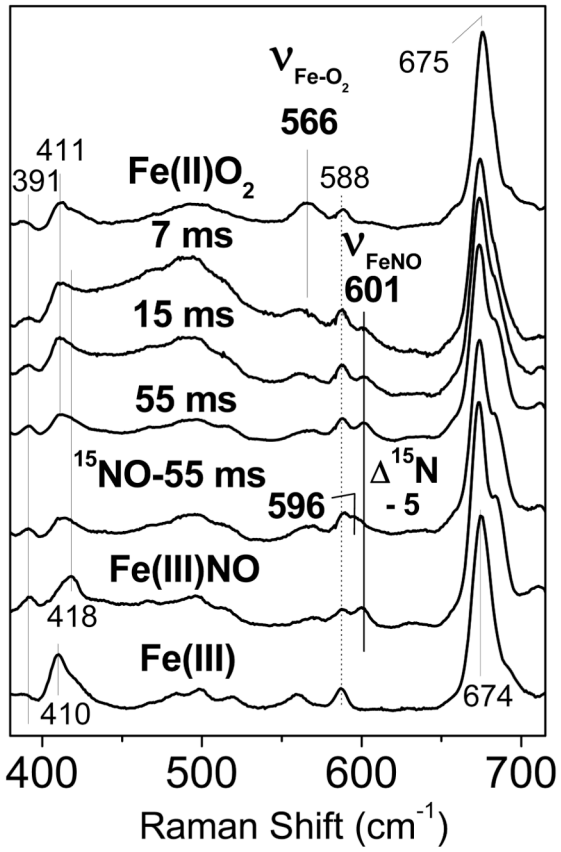

Figure 3.

Low-frequency RR spectra of RFQ samples of the reaction of 300 μM oxy-DevS with excess NO compared to those of resting oxy- (top trace), and Fe(III)NO-DevS and Fe(III)-DevS (bottom two traces). The spectrum of an RFQ sample frozen after 55 ms for the same reaction, but with excess ^{15}NO is also shown (λ_{exc} = 413 nm, 20 mW; sample temperature ~105 K).

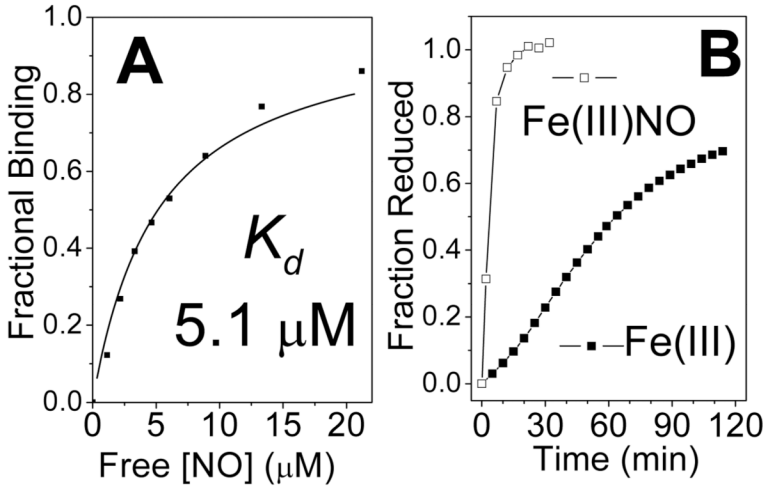

Figure 4.

Binding curve determined from the titration of anoxic Fe(III)-DevS with NO (A), and reduction time course of 4.5 μM Fe(III)-DevS with 10 mM ascorbate in the presence and absence of 25 μM NO (B).

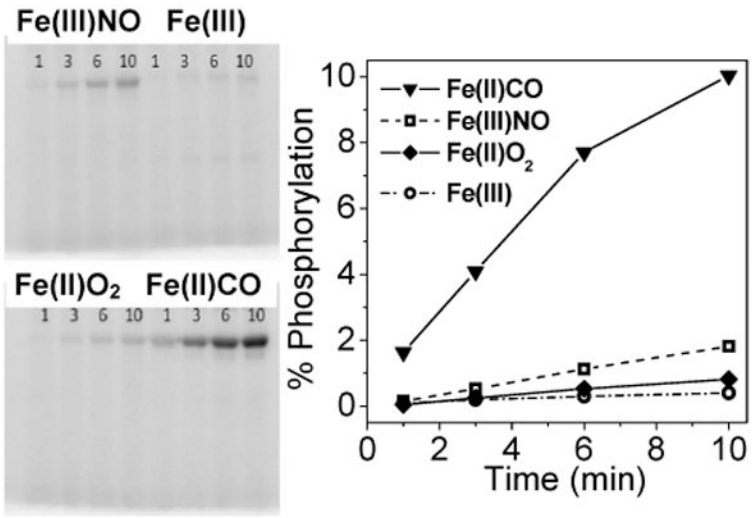

Figure 5.
Autophosphorylation of 5 μM DevS in the presence of 500 μM ATP.

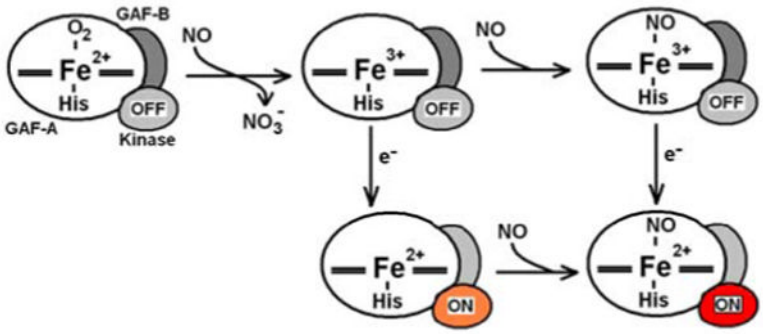

Figure 6.

Proposed mechanism of kinase activation in the reaction of oxy-DevS with NO. The kinase domain is color grey when inhibited, orange for the intermediate autokinase activity observed in deoxy-DevS, and red for the full activation observed with the Fe(II)-NO complex.

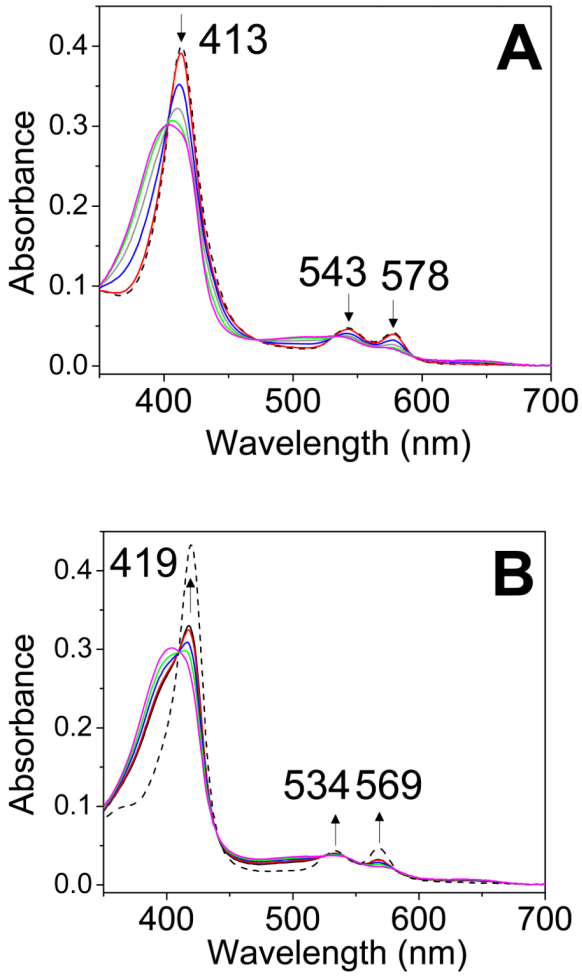

Figure 7.

Room temperature time course of the reaction of oxy-DosT with 1.33 equiv of DEA-NONOate at pH 7.4 (DEA-NONOate generates 1.5 equiv NO with a $t_{1/2}$ ~ 16 min). Panel A shows the first 21 minutes of the reaction while panel B corresponds to the subsequent 30 minutes. Reference spectra of oxy-DosT (A) and DosT Fe(III)-NO (B) are also shown (black dashed lines).